UNIVERSITÄT AUGSBURG
Universitätsbibliothek

OPEN ACCESS
OPUS AUGSBURG

Aging and regeneration of Pt/TiO2 oxidation catalysts for methanol fueled marine engines

Erika Croner, Franz Koschany, Marian Schenker, Stephan Glamsch, Hans-Philipp Walther, Olaf Hinrichsen

Angaben zur Veröffentlichung / Publication details:

Croner, Erika, Franz Koschany, Marian Schenker, Stephan Glamsch, Hans-Philipp Walther, and Olaf Hinrichsen. 2026. "Aging and regeneration of Pt/TiO2 oxidation catalysts for methanol fueled marine engines." *Fuel Communications* 28 (September): 100159. https://doi.org/10.1016/j.jfueco.2026.100159.

Nutzungsbedingungen / Terms of use:

CC BY 4.0

Dieses Dokument wird unter folgenden Bedingungen zur Verfügung gestellt: / This document is made available under these conditions:
CC-BY 4.0: Creative Commons: Namensnennung
Weitere Informationen finden Sie unter: / For more information see:
https://creativecommons.org/licenses/by/4.0/deed.de

Fuel Communications 28 (2026) 100159

Contents lists available at ScienceDirect

Fuel Communications

journal homepage: www.sciencedirect.com/journal/fuel-communications

Aging and regeneration of Pt/TiO_2 oxidation catalysts for methanol fueled marine engines☆

Erika Croner [a,b,*], Franz Koschany [b], Marian Schenker [b], Stephan Glamsch [c], Hans-Philipp Walther [b], Olaf Hinrichsen [a]

[a] Department of Chemistry, TUM School of Natural Science and Catalysis Research Center, Technical University of Munich, Lichtenbergstraße 4, 85748 Garching, Germany

[b] Everllence SE, Stadtbachstraße 1, 86153 Augsburg, Germany

[c] Institute of Physics, University of Augsburg, Universitätsstraße 1, 86159 Augsburg, Germany

ARTICLE INFO

Keywords:
Methanol
Pt/TiO_2
Regeneration
Hydrothermal
Sulfur aged
Field aged

ABSTRACT

The reduction of greenhouse gases is an important and global topic. The maritime sector significantly contributes to global greenhouse gas emissions. To mitigate these emissions, renewable and environmentally friendly fuels such as green methanol (MeOH) can be utilized. However, to reduce toxic and environmentally harmful emissions, MeOH fueled engines require an oxidation catalyst which is able to maintain sufficient high activity under hydrothermal stress and exposure to sulfur. We investigate for the first time the degradation behavior of a Pt/TiO_2 oxidation catalyst under four distinct aging conditions (thermal, hydrothermal, sulfur and field aging) by using the exhaust gas composition of a MeOH engine. A comparison of these aging effects, including their dependence on Pt loading, is presented. Unexpectedly, sulfur and field aged Pt/TiO_2 oxidation catalysts exhibited enhanced NO oxidation activity, revealing a previously unreported aging-induced catalytic behavior. In addition, the sulfur and field aged oxidation catalysts were regenerated using the exhaust gas composition of a MeOH engine. Moreover, the impact of different gas compositions in the exhaust gas of a MeOH engine on the regeneration effect was evaluated. Finally, characterization analyses were conducted to correlate catalytic performance with physicochemical changes induced by aging and regeneration. Our findings provide new insights into degradation and regeneration behavior of Pt/TiO_2 catalysts under realistic MeOH marine engine conditions and contribute to the development of the exhaust aftertreatment system of a MeOH fueled engine. The development is particularly supported by the unexpected aging-induced enhancement of NO oxidation activity.

1. Introduction

One of the most important global challenges is the preservation of the environment and atmosphere. The shipping industry contributes to approximately 2% of global CO_2 emissions (2024), 13% of all SO_2 and 12% of all NO_2 emissions (2017) worldwide [1,2]. Although the use of renewable energy is increasing in Europe, global greenhouse gas emissions continue to rise [3–5]. One approach to reduce these emissions is by the adoption of green fuels in the maritime industry, such as methanol (MeOH). Accordingly, this study applies a green approach based on catalysis and regeneration strategies to reduce hazardous emissions, in accordance with the principles of red chemistry [6].

MeOH combustion is expected to produce fewer environmental harmful emissions, compared to diesel [7]. Furthermore, MeOH exhibits a high biodegradability, which is an important safety factor in case of fuel leakage. It is also easy to handle due to its liquid state at room temperature [8,9].

However, MeOH also has some disadvantages compared to diesel, including lower energy density, reduced lubricity, material compatibility challenges and a low flash point, which poses storage and safety concerns. Additionally, MeOH burns with an almost invisible flame, further posing a safety risk [7,9]. Despite these disadvantages, MeOH remains a promising alternative fuel due to its logistical advantages, renewable production and expected combustion emissions.

☆ This article is part of a Special issue entitled: 'ASICI 2025' published in Fuel Communications.

* Corresponding author at: Department of Chemistry, TUM School of Natural Science and Catalysis Research Center, Technical University of Munich, Lichtenbergstraße 4, 85748 Garching, Germany.

E-mail address: erika.croner@tum.de (E. Croner).

https://doi.org/10.1016/j.jfueco.2026.100159
Received 11 January 2026; Received in revised form 25 May 2026; Accepted 12 June 2026
Available online 13 July 2026
2666-0520/© 2026 The Authors. Published by Elsevier Ltd. This is an open access article under the CC BY license (http://creativecommons.org/licenses/by/4.0/).

MeOH oxidation partly yields formaldehyde (HCHO) formation, a compound known for its toxicity and harmful environmental impact [10,11]. For safety reasons, MeOH engines have to be dual fuel capable. When operating with an oxidation catalyst and MeOH/diesel blends, NO_2 can be formed, which is harmful to human health and environment [12,13]. In addition, it is associated with visible exhaust plumes [14].

To minimize undesired emissions of certain engines operating with diesel and MeOH, a system comprising a selective catalytic reduction (SCR) catalyst and an oxidation catalyst is necessary [10,15]. Typically, for the SCR system a vanadium-, tungsten- and titanium oxide (VTT) catalyst is used due to its hydrothermal (HTA) and poison stability [16–19].

The oxidation catalyst has to be resistant toward HTA aging and sulfur exposure, especially when located upstream of the SCR catalyst or when operating with high sulfur diesel fuels. Previous studies have shown that sulfur poisoning is one of the major catalyst deactivation factors [20]. SO_2 is known to be adsorbed onto active noble metal sites, thereby impairing the adsorption of other reactants, consuming oxygen competitively, hindering the dissociative adsorption of O_2 and thus deteriorating catalyst performance [21–24]. Moreover, SO_2 adsorption can block pores and induce recrystallization of noble metal facets, reducing catalytic reactivity [25–27].

However, some studies have also reported an enhancement of the oxidation activity after S aging for specific reaction species. Ladolcetta [25] observed a promoting effect of SO_2 exposure on the oxidation of C_2H_6, C_3H_8 and n-C_4H_{10} over various noble metal catalysts, while a deterioration of CH_4 and CO oxidation activity was noted. The observed enhancement was attributed to the formation of new active sites associated with the formation of sulfate species as well as SO_2 induced Pt particle growth. Similarly, Chen et al. [28] reported an increased C_3H_8 conversion over a Pt/TiO_2 oxidation catalyst when S is present in the feed gas. The improved activity was explained by the formation of (Pt–S–O)–Ti structures.

Usually, HTA aging also leads to activity loss in precious metal oxidation catalysts. Some reasons for the degradation include thermal induced sintering of active metals, change in Pt oxidation state, phase transitions of the support and loss of specific surface area [29–32]. For instance, TiO_2 can undergo a phase transformation from anatase to rutile, resulting in reduced catalytic activity [33,34].

For this study, Pt/TiO_2 was selected as oxidation catalyst due to its well-known sulfur resistance. Pt is generally considered more sulfur tolerant than Pd [35]. In addition, TiO_2 forms thermally unstable sulfates, which further enhances sulfur resistance [36]. Moreover, Pt/TiO_2 exhibits strong metal–support interactions (SMSI), which help stabilize highly dispersed Pt sites [37].

The promoting or inhibiting effect of sulfur poisoning has been studied by the oxidation of hydrocarbons such as C_3H_6, C_2H_6, C_3H_8, n-C_4H_{10}, C_6H_{14}, C_2H_4, CH_4, as well as NO and CO [24,25,38–42]. Thereby, sulfur exposure of a Pt/Al_2O_3 was found to decrease the oxidation potential of NO [38]. Similarly, HTA aging effects have been examined among others by the oxidation of NO, NH_3, CO and C_3H_6 [29–32,34].

TA, HTA, S and field aging is hypothesized to significantly affect the oxidation behavior of Pt/TiO_2 catalysts under MeOH engine exhaust conditions [34,38,43]. Also, the change is expected to strongly depend on the active metal loading [44]. Furthermore, catalyst regeneration after S aging using MeOH engine exhaust is hypothesized to partially restore catalytic activity [38]. The investigation of these presumptions is crucial and would offer valuable insights for the development of the exhaust aftertreatment system for MeOH fueled marine engines.

To date, however, no studies have investigated the effects of thermal (TA), HTA, S or field aging of a Pt/TiO_2 oxidation catalyst using the exhaust gas composition of a MeOH engine. In particular, how the oxidation capacity is affected for NO, MeOH and HCHO by S and field aging. Furthermore, for the first time a direct comparison of these aging effects has been presented, including their variation across different active metal loadings. Additionally, S and field aged catalysts have been regenerated using the exhaust gas of a MeOH engine, which has not been reported before. Moreover, the influence of different gas compositions in the exhaust gas of a MeOH engine on the regeneration process has been evaluated. The analytical data have further enabled the correlation between physicochemical changes with catalytic performance.

2. Experimental setup

Experiments were conducted on a synthetic gas test bench. Adjustable gas concentrations were passed through a reactor at a defined temperature and subsequently analyzed using a Fourier-transform infrared (FTIR) spectrometer (model type: MKS MultiGas FTIR Analyzer 2030 5 Hz). Each measurement step was held for approximately 30 min to achieve thermal equilibrium across the catalyst. For data evaluation the last 100 data points were considered, recorded at a rate of 1 value every 2 s. The investigated oxidation catalysts were metallic substrates coated with a Pt/TiO_2 washcoat and were acquired commercially.

The feed gas used in this study originated from an engine operating with MeOH and consisted of 1000 ppm MeOH, 1000 ppm CO, 750 ppm NO, 10% H_2O and 12% O_2. During all experiments a nitrogen balance was maintained. The conversion of NO was calculated according to Eq. (1). The conversions of MeOH and CO were determined using the same approach. The yield of HCHO was obtained using Eq. (2). The term "inlet" refers to the feed gas introduced to the reactor, while "outlet" indicates the gas composition measured downstream of the catalyst.

$$X_{NO} = \frac{[NO_{inlet}] - [NO_{outlet}]}{[NO_{inlet}]} \quad (1)$$

$$Y_{HCHO} = \frac{[HCHO_{outlet}]}{[MeOH_{inlet}]} \quad (2)$$

For TA aging experiments, catalysts were heated up to 550 °C and held for 100 h under an air gas flow. Temperatures of this magnitude can appear in the exhaust aftertreatment of engines under certain abnormal but realistic conditions, such as engine misfires, air–fuel issues, problems with back pressure or incorrect ignition timing [45–47]. The selected aging duration was based on typical operating lifetimes of exhaust aftertreatment systems while considering that such elevated temperatures are expected to occur only under exceptional operating conditions. For HTA aging experiments, catalysts were similarly heated to 550 °C for 100 h while being exposed to a gas mixture containing 10% H_2O and 12% O_2. The catalyst activities were measured sequentially before and after the TA and HTA aging procedures. Additionally, to monitor the aging progression a reference point was recorded periodically at 350 °C and with a higher space velocity (SV) compared to the other experiments presented in this work. The SV was increased to enhance the detectability of potential changes in catalyst performance.

For sulfur poisoning experiments, 100 ppm SO_2, 10% H_2O and 12% O_2 were fed through the oxidation catalyst at 350 °C for 100 h. In total, the catalyst was exposed to 1.2 liter SO_2 at 350 °C and atmospheric pressure. This amount and aging temperature are typical for engine operating conditions.

For field aged investigations, a catalyst sample was aged for 1800 operating hours aboard a real ship running with distillate marine fuel (DMA). Upon catalyst removal, fuel oil, lube oil and urea samples were collected and analyzed to identify potential catalyst poisons (see Table S 1). The fuel sample contained approximately 0.1 wt% S, the lube oil exhibited elevated P and Zn concentrations and the urea solution showed significant levels of S, Ca, Na, Al, K and Cl. After S and field aging, a regeneration protocol was applied. The regenerated S and field aged samples will be further referred to as SR and FR, respectively. Subsequently, the catalytic activity was recorded and compared with

Table 1
Different gas mixtures used for the regeneration of S aged oxidation catalysts.

Abbreviation	Regeneration gas mixture	x_0	x_1	x_2	x_3
R MeOH	x ppm MeOH, 1000 ppm CO, 750 ppm NO, 10% H_2O, 12% O_2	N/A	500 ppm	1000 ppm	2000 ppm
R CO	x ppm CO, 750 ppm NO, 10% H_2O, 12% O_2	N/A	500 ppm	1000 ppm	2000 ppm
R NO	x ppm NO, 10% H_2O, 12% O_2	N/A	250 ppm	750 ppm	1250 ppm
R H_2O	x% H_2O, 12% O_2	0%	5%	10%	15%

the average activity determined from multiple experiments with the fresh catalyst.

The SR and FR samples were regenerated by using the exhaust gas derived from the MeOH engine and the temperature program illustrated in Fig. 1(a). To enable the immediate detection of activity changes, the temperature was increased in steps of 10 °C every 60 s until reaching 400 °C (R 400 °C). Upon reaching this temperature the catalyst was held at 400 °C for 2 h while maintaining a constant gas flow. Subsequently, the catalyst was again cooled to 200 °C and then reheated to 450 °C (R 450 °C) and finally to 500 °C (R 500 °C). To investigate potential time dependency, the catalyst was repeatedly cooled and reheated to 500 °C in four consecutive cycles.

To evaluate the influence of different aging conditions on the platinum content, samples with varying Pt loadings ((x, x+5, x+22) g/ft^3 Pt) were analyzed. However, the majority of experiments and analyses reported in this study were conducted using a catalyst with a Pt loading of x+5 g/ft^3. Variations in Pt loading were employed solely to investigate their effect on different aging methods.

Next, the impact of adding individual gas species to a base gas mixture as well as their concentrations and exposure times on the regeneration process were examined. Therefore, a reference point was established at 350 °C and measured before and after each regeneration step, as shown in Fig. 1(b). The reference steps were measured using the exhaust derived gas mixture from the MeOH engine. The first regeneration steps were conducted at 400 °C, followed by 450 °C and finally 500 °C. Each regeneration step was maintained at the specified temperature for 2 h. The regeneration was first conducted using a MeOH, CO, NO, H_2O and O_2 containing gas mixture (R MeOH) and subsequently with modified mixtures: without MeOH (R CO), without MeOH and CO (R NO) and without MeOH, CO as well as NO (R H_2O) (Table 1). Additionally, the concentrations of MeOH (in R MeOH), CO (in R CO), NO (in R NO) and H_2O (in R H_2O) were varied (Table 1). However, the x_0 variation was only done for R H_2O. Furthermore, to ensure better comparability between the differently regenerated catalysts, the catalytic activity was normalized to a similar S aged activity. All regeneration and aging steps were done at a lower SV compared to the activity measurements in this work.

To elucidate catalyst aging behavior, several analytical techniques were conducted. Prior to the experiments, the washcoat was mechanically separated from the metallic substrate. First, X-ray fluorescence (XRF) experiments were performed. To obtain reliable results each sample was measured three times.

Furthermore, Brunauer–Emmett–Teller (BET) surface area and Barrett–Joyner–Halenda (BJH) pore size distribution analyses were carried out. Prior to the measurement, the samples were degassed at 200 °C under vacuum overnight. The complete N_2 adsorption and desorption isotherms were recorded. The BET surface areas were calculated using the relative pressure range of (0.05 – 0.3) p/p_0. Each experiment was repeated several times using different portions of powder from the same sample to ensure statistical reliability.

The metal dispersion (D_M) was calculated using Eq. (3) [48–50].

$$D_M = \frac{[K \cdot V_{B,M}]}{[d_M \cdot A_{S,M}]} = \frac{[K \cdot M_M]}{[d_M \cdot A_{S,M} \cdot N_A \cdot \rho_M]} \quad (3)$$

D_M is inversely proportional to the metal particle diameter (d_M). K presents a shape factor (6 for spherical particles). $A_{S,M}$ describes the surface area occupied by a single surface atom, while $V_{B,M}$ represents

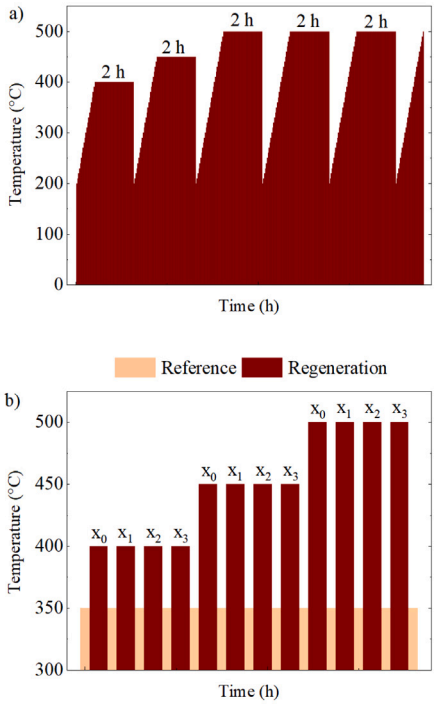


Fig. 1. Temperature procedure for (a) the regeneration process of the SR and FR catalysts and (b) the investigations regarding the influence of the feed gas compositions and concentrations on the regeneration process. The used gas compositions and concentrations (x_0, x_1, x_2 and x_3) are listed in Table 1.

the volume of a bulk metal atom. The latter can be calculated by using the molar mass (M_M), Avogadro's constant (N_A) and the metal density (ρ_M). d_M was determined using a scanning electron microscope (SEM). To ensure representative statistics, SEM images were taken from eight different regions of each catalyst at 100 000 magnification. Figure S 1 shows an exemplary image using a HE-SE2 detector. Due to low contrast between the Pt particles and the washcoat, particle size determination was challenging. To enhance contrast to the Pt particles, we used the Oxford Inst. Unity detector's back-scattered electron (BSE) images. With that, images with sufficient high resolution and element contrast suitable for D_M measurements were obtained.

To examine surface elemental composition, energy dispersive X-ray (EDX) spectroscopy was conducted. Furthermore, to investigate changes in the surface structure X-ray diffraction (XRD) experiments were carried out using an Empyrean diffractometer from Malvern Panalytical. Patterns were collected with a Cu-Kα radiation (λ = 1.5406 Å), a step size of 0.0065° and a step time of 1.4 s.

For thermogravimetric analysis (TGA), the washcoat was degassed in the TGA chamber at 180 °C for one hour under a continuous gas flow. Subsequently, the temperature was elevated to 1000 °C with a heating rate of 10 °C per minute and a gas flow of 12% O_2, 8.6% H_2O and 79.4% N_2. Additionally, the TGA system was connected to an FTIR spectrometer, enabling monitoring of the gas composition downstream of the TGA chamber.

3. Results and discussion

Fig. 2(a) compares the activity of the TA aged catalyst with the fresh catalyst, showing almost no difference in catalytic activity. Relative to the fresh catalyst D_M is reduced (Table 2). This reduction is most likely associated with sintering effects, which do not significantly influence the catalyst's activity. Furthermore, no phase transition or change in the crystal structure of the support is observed in any of the aged samples (Figure S 3). However, an increase in the Pt(111) and Pt(200) reflection intensity is detected between the fresh and all aged samples, which can be attributed to enhanced crystallinity or crystal growth. Given that the TA aged sample exhibits no change in catalytic performance, the enhanced crystallinity or crystal growth is unlikely to have a considerable impact on the activity of the other aged catalysts. TA aging of Pt/TiO_2 catalysts has previously been reported in literature. However, the applied aging conditions, particularly the temperature and gas composition, were not representative for MeOH engine applications, making a direct comparison challenging. Nevertheless, similar changes in the intensities of the Pt(111) and Pt(200) reflections as well as an increase in Pt particle size were observed [43].

For the HTA aged catalyst, the yield and conversions remain unchanged for most of the gas species compared to the fresh catalyst (Fig. 2(b)). Only NO presents a lower conversion to NO_2, indicating a partial loss in oxidation activity. The highest rate of activity loss occurs within the first 10 h of treatment. Subsequently, the oxidation activity decreases continuously (Figure S 2). HTA aging occurs when the exhaust gas system is exposed to temperatures of 550 °C or larger in the presence of water vapor. The resulting lower NO_2 formation is considered beneficial.

Similar to the TA aged catalyst, a reduction in the metal dispersion D_M is observed for the HTA aged catalyst. Since this reduction is similar to that observed in the TA aged catalyst, it is not expected to contribute significantly to the activity loss. The slight reduction in BET surface area and BJH pore volume, attributed to minor sintering effects, could contribute to the activity loss. However, the change in BJH pore volume lies within the experiential uncertainty and thus cannot be confirmed definitively. A change in the oxidation state of the Pt sites is another possible explanation for the decrease in NO oxidation potential, as proposed by Dadi et al. [31]. Previous studies have investigated the HTA aging of a Pt/TiO_2 catalyst. However, the applied gas composition and aging temperature were not representative for MeOH engine operating conditions, making a direct comparison difficult. Nevertheless, the reported aging resulted in Pt particle growth and decreased surface area, which is in agreement with the structural changes observed in our study [34].

After S aging and subsequent regenerating (SR), the catalyst showed a notable increase in NO oxidation potential. In contrast, only a slight increase in HCHO oxidation was observed, while CO and MeOH oxidation remained largely unchanged (Fig. 2(c)).

As expected, the sulfur content is considerably higher in the S aged catalyst compared to the fresh sample (Table 2). The BET surface area shows a slight decrease compared to the fresh catalyst. However, this change lies within the range of experimental uncertainty (Table 2). Similarly, the BJH pore volume remains within the experimental uncertainty. However, the BJH pore size distribution of the S aged catalyst exhibits a shift toward larger pore diameters, suggesting partial sulfur blockage of small pores (Fig. 3). Compared to the fresh catalyst the D_M value shows no meaningful change, remaining within the range of experimental uncertainty. Despite the pore blockage and sulfur poisoning, an increase in oxidation potential is observed. This may be attributed to the formation of (Pt–S–O)–Ti species on Pt and the catalyst support. SO_2 is known to induce oxygen vacancies on the catalyst surface. These vacancies have a strong ability to adsorb oxygen, thereby facilitating the oxidation of SO_2 and leading to the formation of (Pt–S–O)–Ti structures [28]. The oxygen species in these structures provide additional oxidation sites, especially for NO oxidation.

S aging and regeneration have previously been reported for a Pt/Al_2O_3 oxidation catalyst. After a sulfation period of 20 h followed by regeneration with a gas mixture containing C_3H_6, NO, CO, H_2O and O_2, the NO oxidation activity of the fresh catalyst could not be fully restored [38]. However, direct comparison with our study is difficult, as different catalysts and regeneration gas compositions, among other parameters, were employed.

The catalytic behavior of the FR catalyst is similar to the SR catalyst (Fig. 2(d)). It exhibits an increased oxidation potential for NO after aging, while only a slight increase is detected for HCHO and no change for MeOH and CO. XRF analysis of the aged catalyst reveals the presence of P, S and Ca (Table 2). Zinc dialkyldithiophosphate (ZDDP) is a widely used lube oil additive, which is primarily employed for its anti-wear functionality. It can introduce P into the catalyst system [51], leading to deactivation due to its well documented poisoning effects [52,53]. S typically originates from residual impurities in the crude oil [54]. Ca can originate from fuel or lube oil additives that are introduced to bind sulfur [55]. SEM and EDX analyses indicate the presence of $CaSO_4$ residuals on the aged catalyst surface (Figure S 4). $CaSO_4$, phosphate and sulfate deposits can block pores, reducing the BJH pore volume, slightly shifting the BJH pore size distribution toward larger pores and notable decreasing the BET surface area (Table 2 and Fig. 3). In addition, a reduction in the metal dispersion D_M value is observed. However, since it lies within the same range as the TA aged catalyst, no impact on catalyst activity is expected.

Despite metal poisoning and the reduction in specific surface area and BJH pore volume, the formation of (Pt–S–O)–Ti structures [28] are sufficient to enhance the oxidation potential, especially for NO oxidation (Fig. 2).

The regeneration procedures for the SR and FR catalysts were carried out as depicted in Fig. 1(a). The catalytic activity for each temperature cycle is presented in Fig. 4. During the initial temperature increase to 400 °C (R 400 °C) the S and field aged catalysts exhibit lower activities compared to the fresh reference. In the subsequent cycles to higher temperatures, an increase in catalytic performance is observed. The highest activity is achieved in the R 500 °C cycle, exceeding that of the fresh catalyst. Additional cycles at 500 °C do not lead to significant changes in catalyst activity. Most likely some (Pt–S–O)–Ti structures are formed during S aging at 350 °C. However, the limited formation of (Pt–S–O)–Ti structures makes metal poisoning and pore blocking remaining the dominant effects, leading to a decrease in catalyst activity, as seen in R 400 °C. Higher temperatures (400 °C - 500 °C) promote the formation of the (Pt–S–O)–Ti structures, leading to enhanced catalytic activity. Considering the R 500 °C cycles and the concentration profiles of the regeneration steps (Figure S 7), temperature has a much more significant impact on the formation than time.

Overall, when sulfur contaminated MeOH fuel is used, the NO oxidation capacity can either decrease or increase depending on the catalyst temperature. If the catalyst temperature remains below 350 °C, NO oxidation is expected to be lower than in the initial state. However, at temperatures of 400 °C or higher, NO oxidation increases, resulting in higher NO_2 formation. Exhaust aftertreatment systems are more likely to reach 400 °C than 550 °C during operation. Therefore, the aging-induced increase in NO oxidation should be considered when designing exhaust aftertreatment systems for MeOH fueled engines.

The catalysts mentioned until now had a x+5 g/ft^3 Pt loading. Next, we investigated the influence of the Pt content on the catalytic activity for the fresh and differently aged catalysts (Fig. 5). The fresh catalysts show no significant variation in activity. However, after aging, differences emerge. For the HTA aged catalyst, a lower Pt content results in a more pronounced decrease of oxidation potential. At lower Pt content, the reduced availability of Pt sites may be less able to compensate for or mitigate the effects of changes in the Pt oxidation state. The reduction in BET surface area may have a bigger impact at lower Pt loadings, as fewer Pt sites are available to compensate for

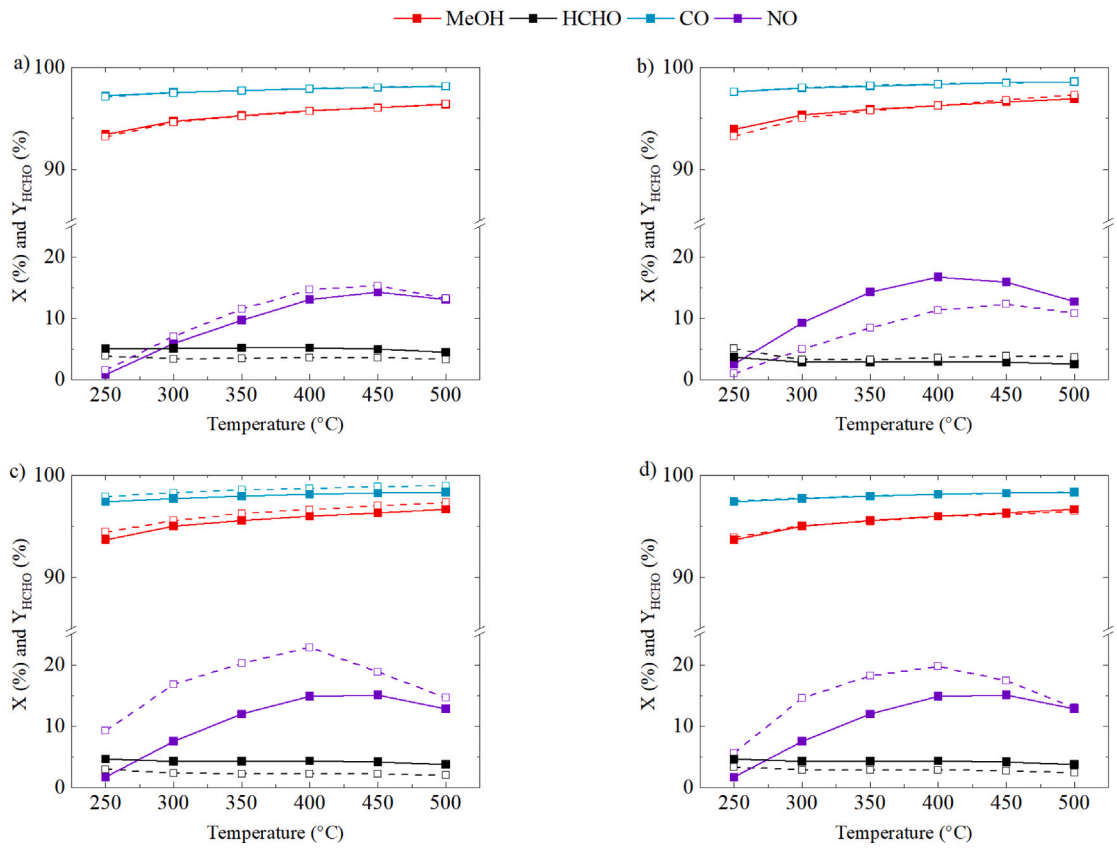


Fig. 2. Comparison of the activity of fresh oxidation catalysts (continuous lines) with that of catalysts aged under different conditions (dashed lines): (a) TA, (b) HTA, (c) SR and (d) FR.

Table 2
XRF, BET and BJH analyses as well as D_M of the fresh and differently aged (TA, HTA, SR, FR) oxidation catalysts.

	P (wt%)	S (wt%)	Ca (wt%)
fresh	0.04 ± 0.004	0.09 ± 0.001	0.03 ± 0.01
TA	0.04 ± 0.01	0.04 ± 0.003	0
HTA	0.04 ± 0.006	0.05 ± 0.04	0.03 ± 0.007
SR	0.05 ± 0.004	0.46 ± 0.02	0
FR	1.26 ± 0.12	0.59 ± 0.03	0.32 ± 0.02
	BET (m^2/g)	BJH pore volume (cm^3/g)	D_M (%)
fresh	103.51 ± 4.06	0.35 ± 0.014	37.38 ± 3.18
TA	90.54 ± 21.2	0.34 ± 0.12	26.73 ± 3.48
HTA	89.81 ± 7.17	0.34 ± 0.0007	27.63 ± 6.24
SR	95.61 ± 9.24	0.37 ± 0.022	33.2 ± 7.45
FR	68.8 ± 9.24	0.28 ± 0.022	22.04 ± 1.59

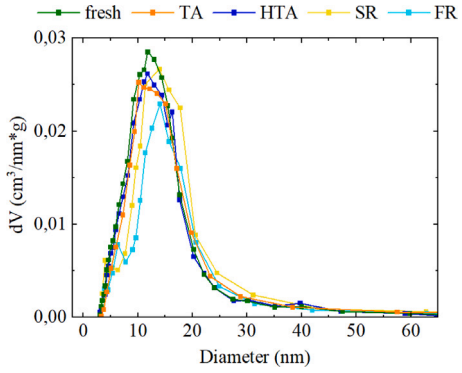


Fig. 3. BJH pore size distribution of oxidation catalysts aged under different conditions (TA, HTA, SR, FR).

it. The SR and FR aged catalysts exhibit an enhancement in oxidation potential at higher Pt loadings (x+5 and x+22 g/ft^3 Pt) compared to the fresh catalyst. However, at the lowest Pt loading (x g/ft^3 Pt), the oxidation potential decreases. The lower Pt concentration reduces the amount of (Pt–S–O)–Ti formation, with metal poisoning and pore blockage becoming the dominant effects. The highest dependency on Pt content is observed for the FR aged catalyst, followed by the SR aged catalyst, while the HTA aged catalyst exhibits the least impact. This is most likely due to the FR catalyst being altered for a longer time and being exposed to more sulfur and phosphorus compared to the SR sample, as indicated by Table 2.

As shown in Fig. 6(a) sulfur remains bound to the catalyst surface up to approximately 630 °C. The mass loss correlates well with the SO_2 concentration measured by the FTIR spectrometer connected to the TGA exhaust (Fig. 6(b)). The first minimum of the TG derivative corresponds to water desorption. At approximately 770 °C temperature a SO_2 desorption minimum is observed for the SR and FR aged catalyst.

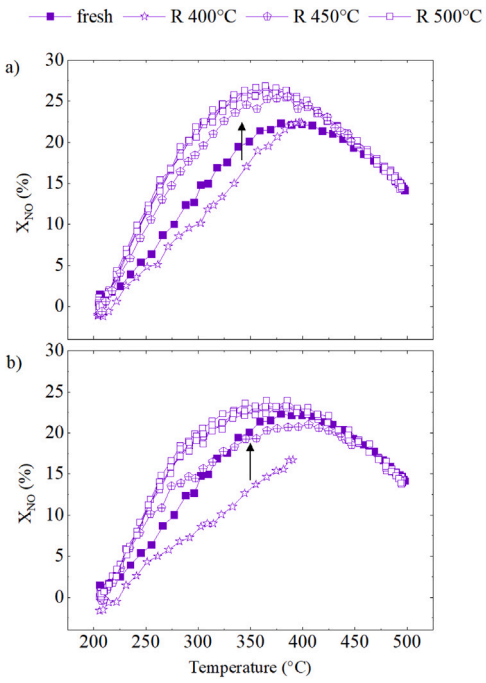


Fig. 4. NO conversion of the regeneration cycles conducted on the S (a) and field aged (b) catalysts, as shown in Fig. 1(a).

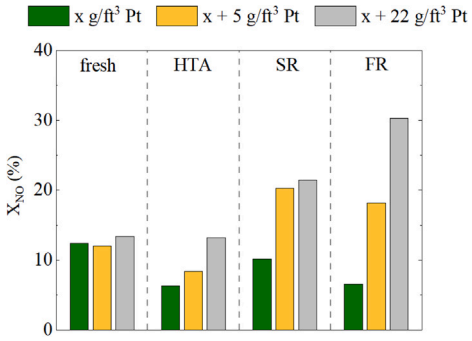


Fig. 5. Impact of Pt content on different aging processes (HTA, SR, FR) at 350 °C.

The FR aged catalyst additionally exhibits a desorption peak at around 860 °C. Typically, bulk $CaSO_4$ exhibits a decomposition temperature above 1100 °C [56]. However, when $CaSO_4$ interacts with the catalyst active sites and undergoes partial reduction, its decomposition temperature can be significantly lowered, approaching the temperature observed in our experiments [57].

Subsequently, the influence of individual gas species, when being added to a gas mixture, and their concentrations on the regeneration process was investigated for the S aged catalyst. The respective activity measurements were normalized to the S aged catalyst before regeneration (Fig. 7). The catalysts treated with the R MeOH, R CO and R H_2O gas mixtures exhibits comparable NO conversion rates. Furthermore, the CO concentration in R CO and the MeOH concentration in R MeOH affect the catalyst performance, with higher concentrations yielding enhanced activity. In contrast, regeneration with the R NO mixture produces only a minimal, nearly negligible change in catalytic activity, independent of the concentration used. Comparable BET surface areas, BJH pore volumes and pore size distributions are observed for the regenerated samples (Table S 2 and Figure S 5). In addition, no differences in their XRD patterns are detected (Figure S 6).

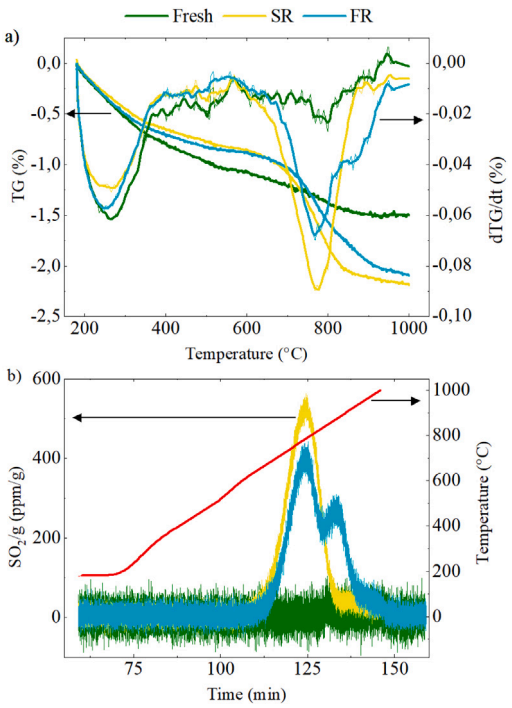


Fig. 6. TGA analysis of the SR and FR aged oxidation catalysts.

The NO oxidation potential increases when regenerating the S aged samples using the R H_2O gas mixture with $x_0 = 0\%$. This indicates that temperature is sufficient for the formation of (Pt–S–O)–Ti structures. Again, time has a minor influence on the formation relative to temperature (Figure S 8). Introducing NO into the gas mixture (R NO) leads to almost no regeneration or enhancement of the oxidation activity. Apparently, the addition of NO inhibits the formation of (Pt–S–O)–Ti structures. In contrast, adding MeOH or CO to the gas mixture causes a pronounced increase in NO conversion. (Pt–S–O)–Ti structures are formed again, thus enhancing the oxidation activity. When MeOH and CO are added to the gas feed, the inhibition is apparently alleviated. Sulfur poisoned Pt oxidation catalysts are known to undergo partial regeneration under reducing atmospheres, which promote the removal of sulfate species from both the support and the Pt surface [58–60]. As CO and MeOH can act as reducing agent, they likely contribute to the depletion of sulfate species [61,62]. Increasing their concentrations enhance sulfate removal, leading to higher NO conversion.

The advanced removal of sulfate by R MeOH and R CO gas mixtures can be proven via TGA and FTIR measurements (Fig. 8). After regeneration, all samples contained less adsorbed sulfur than the S aged catalyst. The S aged sample exhibits two d(TG)/dt minima at approximately 570 °C and 740 °C, corresponding to distinct binding sites. Sulfur species bound to Pt terrace sites desorb around 570 °C, whereas sulfur associated with Pt edge and kink sites desorb at approximately 740 °C [38]. Sulfur adsorbed on terrace sites is completely removed during regeneration, while sulfur bound to edge and kink sites is only partially removed. Adding CO to the gas mixture increased sulfur desorption due to its reducing properties. Introducing MeOH in addition to CO enhanced this effect even further, leading to greater sulfur removal (Fig. 8 and Table S 2).

When sulfur contaminated MeOH fuel is used, the NO oxidation capacity can either decrease or increase depending on the catalyst temperature. If the catalyst temperature remains below 350 °C, NO oxidation is expected to be lower than in the initial state. However, at temperatures of 400 °C or higher, NO oxidation increases, resulting in higher NO_2 formation. Exhaust aftertreatment systems are more likely

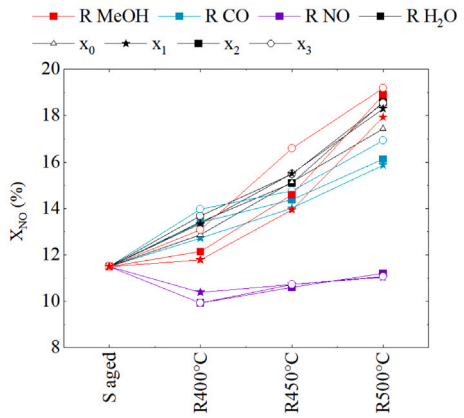


Fig. 7. Impact of different gas mixtures (R MeOH, R CO, R NO, R H_2O) on the regeneration of S aged oxidation catalysts. The regeneration program illustrated in Fig. 1(b) was employed.

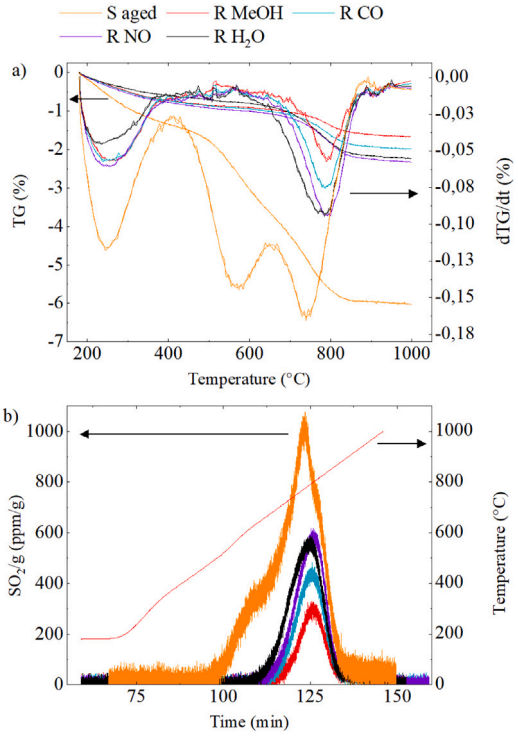


Fig. 8. TGA analysis for the S aged and regenerated (R MeOH, R CO, R NO, R H_2O) oxidation catalysts.

to reach 400 °C than 550 °C during operation. Therefore, the aging-induced increase in NO oxidation should be considered when designing exhaust aftertreatment systems for MeOH fueled engines.

4. Conclusion

Pt/TiO_2 oxidation catalysts were TA, HTA, S and field aged under conditions relevant for MeOH fueled marine engines. The TA aged catalyst exhibited no measurable change in oxidation activity. HTA aging had only a minor influence on MeOH, HCHO and CO oxidation, but significantly reduced the NO oxidation activity. This loss was mainly attributed to a change in the oxidation state of the metal sites.

S and field aged catalysts could be regenerated under the exhaust gas composition of a MeOH engine and even increase their oxidation activity, especially toward NO.

However, MeOH, CO and HCHO oxidation activity was not or only slightly affected. These effects are likely associated with the formation of stable (Pt–S–O)–Ti surface structures involving the Pt sites and the catalyst support. However, the (Pt–S–O)–Ti structures do not form in a NO containing gas mixture (R-NO), resulting in no significant regeneration of catalytic activity.

Overall, no or only minor variations are observed in the oxidation of CO, MeOH and HCHO after TA, HTA, S and field aging. NO oxidation decreases after HTA but increases after S aging. Generally, a decrease in NO oxidation is preferred as NO_2 formation can lead to visible exhaust gas emissions and is harmful to human health and environment.

Finally, this study provides valuable insights into the aging and regeneration behavior of Pt/TiO_2 catalysts and offers guidance for the development of an exhaust aftertreatment system in MeOH fueled engines. Particularly, the observed aging-induced enhancement in NO oxidation activity has to be considered in the aftertreatment design. Overall, the transition toward low-emission maritime transportation is supported. Future studies should further investigate the mechanistic origin of the enhanced NO oxidation activity. Additionally, the impact of different sulfur concentration and fuel impurities on catalyst performance and regeneration should be investigated.

CRediT authorship contribution statement

Erika Croner: Writing – review & editing, Writing – original draft, Visualization, Validation, Methodology, Investigation, Formal analysis, Data curation, Conceptualization. **Franz Koschany:** Writing – review & editing, Supervision. **Marian Schenker:** Writing – review & editing, Resources. **Stephan Glamsch:** Writing – review & editing, Investigation. **Hans-Philipp Walther:** Writing – review & editing, Funding acquisition. **Olaf Hinrichsen:** Writing – review & editing, Supervision.

Declaration of generative AI and AI-assisted technologies in the manuscript preparation process

During the preparation of this work the authors used ChatGPT in order to improve readability. After using this tool, the authors reviewed and edited the content as needed and take full responsibility for the content of the published article.

Declaration of competing interest

The authors declare that they have no known competing financial interests or personal relationships that could have appeared to influence the work reported in this paper.

Acknowledgments

We express our gratitude to Professor Sven Kureti and Till Hauswald for their assistance in sulfur aging our samples. Funding from the German Federal Ministry for Economic Affairs and Climate Action, provided on the basis of a decision by the German Bundestag (project no. 03SX585A), is gratefully acknowledged. Erika Croner expresses her sincere gratitude to the TUM Graduate School for additional support.

Appendix A. Supplementary data

Supplementary material related to this article can be found online at https://doi.org/10.1016/j.jfueco.2026.100159.

Data availability

While some of the data is confidential, most of it can be shared upon a reasonable request.

References

[1] Ashraf M, Bocca R. Net-zero industry tracker: 2024 edition. Tech. rep., Geneva, Switzerland: World Economic Forum; 2024.

[2] Ambsdorf J, Engel A, Grabe J, Kronfeld-Goharani U, Latif M, Lenz M, Lotze H, Matz-Lück N, Müller A, Neumann B. Meeresatlas: Daten und Fakten über unseren Umgang mit dem Ozean. Heinrich Böll Stiftung; 2017.

[3] Jenei S, Módosné Szalai S, Sárközy H, Dhruv PS, Pojda-Noszik N, Kálmán BG, Dávid LD. Europe's energy shift: From fossil fuels to renewable energy. Emerg Sci J 2025;9(5).

[4] Devianto D, Saputra R, Yollanda M, Maiyastri M, Asdi Y, Permana D, Herdiani E. The BVAR model for analyzing CO_2 emissions on renewable energy, economic growth, and forest area. Emerg Sci J 2025;9(3):1158–73.

[5] Crippa M, Guizzardi D, Pagani F, Banja M, Muntean M, Schaaf E, Becker W, Monforti-Ferrario F, Quadrelli R, Risquez Martin A. GHG emissions of all world countries. Publ Off Eur Union, Luxemb 2023;10:953322.

[6] Fegade SL. Red chemistry: Principles and applications. Next Sustain 2024;4:100048.

[7] Verhelst S, Turner JW, Sileghem L, Vancoillie J. Methanol as a fuel for internal combustion engines. Prog Energy Combust Sci 2019;70:43–88.

[8] Bromberg L, Cheng WK. Methanol as an alternative transportation fuel in the US: Options for sustainable and/or energy-secure transportation. Cambridge, MA: Sloan Automotive Laboratory, Massachusetts Institute of Technology; 2010.

[9] Substance Evaluation Report. Tech. rep. 3, Lodz, Poland: Bureau for Chemical Substances; 2015.

[10] Croner E, Koschany F, Schenker M, Walther H-P, Hinrichsen O. Exhaust gas composition of a combustion engine running with methanol after interacting with a vanadium-tungsten-titanium oxide SCR catalyst. Appl Energy Combust Sci 2025;24:100397.

[11] Worker exposure to formaldehyde and formaldehyde releasers. Tech. rep., Helsinki, Finland: ECHA (European Chemicals Agency); 2019.

[12] Latza U, Gerdes S, Baur X. Effects of nitrogen dioxide on human health: systematic review of experimental and epidemiological studies conducted between 2002 and 2006. Int J Hyg Environ Health 2009;212(3):271–87.

[13] Bashir MR, Alomran M, Gill AN, Tufail Khan QA, Jameel S, Rafiq MU, Khan F. Rising nitrogen dioxide (NO_2): A growing threat to environment and plant health. J Agric Biology 2024;2(1):76–83.

[14] Kotchmar DJ, Garner J, Gardner D, Comfort B. Air quality criteria for oxides of nitrogen. Diane Publishing; 1996.

[15] Croner E, Koschany F, Schenker M, Walther H-P, Hinrichsen O. Evaluation of different exhaust aftertreatment constellations for engines running with Methanol. Chem Eng Res Des 2025;227:677–84.

[16] Lisi L, Cimino S. Poisoning of SCR catalysts by alkali and alkaline earth metals. Catalysts 2020;10(12):1475.

[17] Economidis NV, Peña DA, Smirniotis PG. Comparison of TiO_2-based oxide catalysts for the selective catalytic reduction of NO: effect of aging the vanadium precursor solution. Appl Catal B: Environ 1999;23(2–3):123–34.

[18] Chen H, Xia Y, Fang R, Huang H, Gan Y, Liang C, Zhang J, Zhang W, Liu X. The effects of tungsten and hydrothermal aging in promoting NH_3-SCR activity on V_2O_5/WO_3-TiO_2 catalysts. Appl Surf Sci 2018;459:639–46.

[19] Marberger A, Elsener M, Ferri D, Kröcher O. VO_x surface coverage optimization of V_2O_5/WO_3-TiO_2 SCR catalysts by variation of the V loading and by aging. Catalysts 2015;5(4):1704–20.

[20] Wang L, Huang C, Gao Z, Cui B, Zhao M, Xiao M, Yu X. Recent Research on the Anti-Poisoning Catalysts in the Catalytic Oxidation of VOCs: A Review. Catalysts 2025;15(3):234.

[21] Li L, Shen Q, Cheng J, Hao Z. Catalytic oxidation of NO over TiO_2 supported platinum clusters. II: Mechanism study by in situ FTIR spectra. Catal Today 2010;158:361–9.

[22] Franken T, Vieweger E, Klimera A, Hug M, Heel A. Sulphur tolerant diesel oxidation catalysts by noble metal alloying. Catal Commun 2019;129:105732.

[23] Gracia F, Guerrero S, Wolf E, Miller J, Kropf A. Kinetics, operando FTIR, and controlled atmosphere EXAFS study of the effect of sulfur on Pt-supported catalysts during CO oxidation. J Catalysis 2005;233(2):372–87.

[24] Kummer J. Laboratory experiments evaluating the effects of S and Cu on a Pt Al_2O_3 auto exhaust oxidation catalysts. J Catalysis 1975;38(1):166–71.

[25] Ladolcetta M. Deactivation and enhancement effects of sulfur on supported platinum oxidation catalysts. New Jersey Institute of Technology; 2000.

[26] Van Spronsen MA, Frenken JW, Groot IM. Surface science under reaction conditions: CO oxidation on Pt and Pd model catalysts. Chem Soc Rev 2017;46(14):4347–74.

[27] Somorjai G. On the mechanism of sulfur poisoning of platinum catalysts. Lawrence Berkeley National Laboratory; 1972.

[28] Chen W, Zheng J, Fang Y, Wang Y, Hu J, Zhu Y, Zhu X, Li W, Zhang Q, Pan C, Zhang B, Qiu X, Wang S, Cui S, Wang J, Wu J, Luo Z, Guo Y. Role of the in-situ-formed surface (Pt-S-O)-Ti active structure in SO_2-promoted C_3H_8 combustion over a Pt/TiO_2 catalyst. Environ Sci Technol 2024;58(6):3041–53.

[29] Dhillon PS, Harold MP, Wang D, Kumar A, Joshi S. Hydrothermal aging of Pt/Al_2O_3 monolith: Washcoat morphology degradation effects studied using ammonia and propylene oxidation. Catal Today 2019;320:20–9.

[30] Schuetz J, Stoermer H, Lott P, Deutschmann O. Effects of hydrothermal aging on CO and NO oxidation activity over monometallic and bimetallic Pt-Pd catalysts. Catalysts 2021;11(3):300.

[31] Dadi RK, Daya R, Kumar A, Joshi SY, An H, Cunningham MJ, Currier NW, Yezerets A. A modeling and experimental study on hydrothermal aging deactivation of NO oxidation activity on Pt-Pd catalyst. Appl Catal B: Environ 2021;283:119655.

[32] Ogel E, Casapu M, Doronkin D, Popescu R, Stormer H, Mechler C, Marzun G, Barcikowski S, Türk M, Grunwaldt J-D. Impact of preparation method and hydrothermal aging on particle size distribution of Pt/γ-Al_2O_3 and its performance in CO and NO oxidation. J Phys Chem C 2019;123(9):5433–46.

[33] Porter JF, Li Y-G, Chan CK. The effect of calcination on the microstructural characteristics and photoreactivity of Degussa P-25 TiO_2. J Mater Sci 1999;34(7):1523–31.

[34] Yang Z, Zhang N, Cao Y, Li Y, Liao Y, Li Y, Gong M, Chen Y. Promotional effect of lanthana on the high-temperature thermal stability of Pt/TiO_2 sulfur-resistant diesel oxidation catalysts. RSC Adv 2017;7(31):19318–29.

[35] Wilburn MS, Epling WS. Formation and decomposition of sulfite and sulfate species on Pt/Pd catalysts: An SO_2 oxidation and sulfur exposure study. ACS Catal 2018;9(1):640–8.

[36] Yang W, Gong J, Wang X, Bao Z, Guo Y, Wu Z. A review on the impact of SO_2 on the oxidation of NO, hydrocarbons, and CO in diesel emission control catalysis. ACS Catal 2021;11(20):12446–68.

[37] Svintsitskiy D, Kibis L, Stadnichenko A, Slavinskaya E, Zaguzin A, Romanenko A, Derevyannikova E, Stonkus O, Boronin A. The influence of the metal-support interaction on the catalytic activity of Pt/Al_2O_3 and Pt/TiO_2 in NH_3 oxidation. AIP Conference Proceedings 2019;2143(1):020028.

[38] Li Y, Shen M, Wang J, Wan T, Wang J. Influence of sulfation and regeneration on Pt/Al_2O_3 for NO oxidation. Catal Sci Technol 2015;5(3):1731–40.

[39] Soloviev SO, Kyriienko PI, Popovych NO. Effect of CeO_2 and Al_2O_3 on the activity of Pd/Co_3O_4/cordierite catalyst in the three-way catalysis reactions (CO/NO/C_nH_m). J Environ Sci 2012;24(7):1327–33.

[40] Huang H, Long R, Yang R. A highly sulfur resistant Pt-Rh/TiO_2/Al_2O_3 storage catalyst for NO_x reduction under lean-rich cycles. Appl Catal B: Environ 2001;33(2):127–36.

[41] Clark PD, Sui R, Dowling NI, Huang M, Lo JM. Oxidation of CO in the presence of SO_2 using gold supported on La_2O_3/TiO_2 nanofibers. Catal Today 2013;207:212–9.

[42] Liotta L, Di Carlo G, Longo A, Pantaleo G, Venezia A. Support effect on the catalytic performance of Au/Co_3O_4-CeO_2 catalysts for CO and CH_4 oxidation. Catal Today 2008;139(3):174–9.

[43] Zhang L, Cheng X, Zhang G, Qiu W, He H, Chen G. High active platinum clusters on titanium dioxide supports toward carbon monoxide oxidation. Appl Catal B: Environ 2020;266:118629.

[44] Yang Y, Fang J, Huang J, Qin Z, Zhang Q, Pu P, Pan S. Influence of different thermal aging conditions on soot combustion with catalyst by thermogravimetric analysis. Materials 2021;14(13):3647.

[45] Prasetyo D. Temperature exhaust gas analysis on the ship engine. J Rekayasa Mesin 2022;13(3):629–35.

[46] Huang L, Liu J, Liu R, Wang Y, Liu L. Experimental investigation on combustion and performance of diesel engine under high exhaust back pressure. Machines 2022;10(10):919.

[47] Ovaska T, Spoof-Tuomi K, Niemi S, Valkjärvi P, Maunula T, Mikulski M, Lehtoranta K, Alanen J, Happonen M. Effect of late diesel injection on close-coupled SCR+ ASC during DPF regeneration period. Fuel 2025;381:133406.

[48] Bui HM, Großmann PF, Berger A, Seidel A, Tonigold M, Szesni N, Fischer R, Rieger B, Hinrichsen O. Comparison of Direct Ink Writing and Binder Jetting for additive manufacturing of Pt/Al_2O_3 catalysts for the dehydrogenation of perhydro-dibenzyltoluene. Chem Eng J 2023;458:141361.

[49] Borodziński A, Bonarowska M. Relation between crystallite size and dispersion on supported metal catalysts. Langmuir 1997;13(21):5613–20.

[50] Rice SB, Chan C, Brown SC, Eschbach P, Han L, Ensor DS, Stefaniak AB, Bonevich J, Vladár AE, Walker ARH. Particle size distributions by transmission electron microscopy: an interlaboratory comparison case study. Metrologia 2013;50(6):663.

[51] Neville A, Morina A. Wear and chemistry of lubricants. Wear - Mater Mech Pr 2005;71–94.

[52] Kärkkäinen M, Kolli T, Honkanen M, Heikkinen O, Huuhtanen M, Kallinen K, Lepistö T, Lahtinen J, Vippola M, Keiski RL. The effect of phosphorus exposure on diesel oxidation catalysts part I: activity measurements, elementary and surface analyses. Top Catal 2015;58(14):961–70.

[53] Ho PH, Shao J, Yao D, Di W, Creaser D, Olsson L. Role of the supports during phosphorus poisoning of diesel oxidation catalysts. Chem Eng J 2023;468:143548.

[54] Shi Q, Wu J. Review on sulfur compounds in petroleum and its products: state-of-the-art and perspectives. Energy & Fuels 2021;35(18):14445–61.

[55] Miyasaka T, Miura K, Hayakawa N, Ishino T, Iijima A, Shoji H, Tamura K, Utaka T, Kamano H. A study on the effect of a calcium-based engine oil additive on abnormal SI engine combustion. SAE Int J Engines 2015;8(1):206–13.

[56] Nielsen AR, Larsen MB, Glarborg P, Dam-Johansen K. High-temperature release of SO_2 from calcined cement raw materials. Energy & Fuels 2011;25(7):2917–26.
[57] Matsuzaki R, Masumizu H, Murakami N, Saeki Y. The thermal decomposition process of calcium sulfite. Bull Chem Soc Japan 1978;51(1):121–2.
[58] Nasri NS, Jones JM, Dupont VA, Williams A. A comparative study of sulfur poisoning and regeneration of precious-metal catalysts. Energy & Fuels 1998;12(6):1130–4.
[59] Jones J, Dupont V, Brydson R, Fullerton D, Nasri N, Ross A, Westwood A. Sulphur poisoning and regeneration of precious metal catalysed methane combustion. Catal Today 2003;81(4):589–601.
[60] Mathieu M-V, Primet M. Sulfurization and regeneration of platinum. Appl Catal 1984;9(3):361–70.
[61] Zhaoliang Z, Jun M, Xiyao Y. Separate/simultaneous catalytic reduction of sulfur dioxide and/or nitric oxide by carbon monoxide over titanium–tin solid solution catalysts. Chem Eng J 2003;95(1):15–24.
[62] Goyal V, Bhatt T, Dewangan C, Narani A, Naik G, Balaraman E, Natte K, Jagadeesh RV. Methanol as a potential hydrogen source for reduction reactions enabled by a commercial Pt/C catalyst. J Org Chem 2023;88(4):2245–59.